Available online at www.sciencedirect.com
SCIENCE DIRECT®
Journal of Nuclear Materials 346 (2005) 145–164
journal of nuclear materials
www.elsevier.com/locate/jnucmat

The influence of fast neutron irradiation and irradiation temperature on the tensile properties of wrought LCAC and TZM molybdenum

B.V. Cockeram [a,*], R.W. Smith [a], L.L. Snead [b]

[a] Bettis Atomic Power Laboratory, Bechtel-Bettis, Inc., P.O. Box 79, West Mifflin, PA 15122-0079, USA
[b] Oak Ridge National Laboratory, P.O. Box 2008, Oak Ridge, TN 37831-6138, USA

Received 8 February 2005; accepted 2 June 2005

Abstract

The effects of irradiation temperature on embrittlement are evaluated by the irradiation of wrought low carbon arc cast (LCAC) and TZM molybdenum in the High Flux Isotope Reactor at 294–1100 °C to neutron doses between 0.6 and 13.1 dpa Mo. Irradiation at 300 °C is shown to result in elevation of the ductile to brittle transition temperature (DBTT) from a pre-irradiated value of −100 to −50 °C to a post-irradiated value of 800 °C for both alloys with an increase in fracture stress. Irradiation at 560 °C also resulted in an increase in fracture stress, but the post-irradiated DBTT for LCAC (300 °C) was much lower than TZM (700 °C). Irradiation of both LCAC and TZM between 935 °C and 1100 °C resulted in little radiation hardening and a −50 °C DBTT for both alloys. The finer grain size and absence of coarse carbide particles may explain the slightly improved embrittlement resistance of LCAC compared to TZM for 600 °C irradiations.

1. Introduction

Molybdenum is a refractory metal that has high strength and creep resistance at high temperatures, as well as possessing high thermal conductivity, and measurable tensile ductility, which are desired properties for many advanced applications [1–8]. Two commercially available molybdenum alloys are: (1) low carbon arc cast (LCAC), which is unalloyed molybdenum with low levels of oxygen and nitrogen, and controlled amounts of carbon [9], and (2) TZM molybdenum, which is alloyed with small amounts of titanium, zirconium, and carbon to produce a coarse distribution of carbides with some titanium and zirconium in solid solution [9]. High amounts of tensile ductility are typically observed in molybdenum-base alloys at low temperatures only when the grain size is fine, the oxygen content is low, and the ratio of carbon to oxygen is high [10–17]. Additions of carbon to unalloyed molybdenum have been shown to decrease the overall oxygen content in the alloy, prevent segregation of oxygen to the grain boundaries to minimize embrittlement, and result in the formation of carbides that strengthen grain boundaries. The presence of coarse (Ti, Zr)-rich carbides together with titanium and zirconium in solution results

* Corresponding author. Tel.: +1 412 476 5647; fax: +1 412 476 5779.
E-mail address: cockeram@bettis.gov (B.V. Cockeram).

0022-3115/$ - see front matter © 2005 Elsevier B.V. All rights reserved.
doi:10.1016/j.jnucmat.2005.06.016

in higher creep resistance and strength for TZM molybdenum at high temperatures.

One concern associated with the irradiation of molybdenum, regardless of its good behavior in the unirradiated condition, is the loss of ductility resulting from irradiation hardening that could increase susceptibility to brittle fracture. This irradiation embrittlement is thought to result from the formation of a high number density ($>10^{13}/cm^3$) of point defect clusters, which increases the flow stress of the material to levels that are higher than the inherent fracture stress [1–8]. A common measure of embrittlement is the change in the ductile to brittle transition temperature (DBTT). The majority of irradiated tensile data indicates that the largest increase in the DBTT of unalloyed molybdenum is observed after irradiation at temperatures $\leqslant$600 °C, although embrittlement for some molybdenum alloys has been reported to occur at irradiation temperatures as high as 800 °C [1–8,18–31]. The Stage V recovery temperature for prominent vacancy diffusion in molybdenum is 600 °C, which identifies this temperature as the lower bound for the irradiation temperature below which embrittlement is expected to be a concern in a material that was not specifically engineered for embrittlement resistance. Slow kinetics for the coarsening and annihilation of the defects that restrict dislocation motion and lead to embrittlement at temperatures just above 600 °C likely explains why irradiation embrittlement can be observed at irradiation temperatures as high as 800 °C in some cases. Microstructural variables such as finer grain size (to absorb point defects), lower interstitial content (to impede cluster nucleation), and alloying elements (to modify point defect diffusion) have been shown to mitigate irradiation embrittlement [1–5,8,18]. Irradiation at temperatures greater than 800 °C provides enough thermal activation for annihilation of the point defects produced by neutron irradiation, which generally results in the formation of a lower number density of coarse voids that result in little change in properties.

The purpose of this work is to determine the change in the tensile properties of wrought LCAC and TZM molybdenum flat products that have a fine-grain size. The influence of composition, microstructure, irradiation temperature and fluence was studied by comparing results for both alloys. This work builds on the results from an earlier paper [3], where LCAC molybdenum was irradiated to fluences between 10.5 and 61.3×10^{24} n/m^2 ($E > 0.1$ MeV), or 0.6 and 3.3 dpa, by reporting results for higher dose irradiations (232–247×10^{24} n/m^2 or 12.3–13.1 dpa).

2. Materials and experimental procedure

Compositions for LCAC sheet (0.508 mm thick) and TZM plate (6.35 mm) obtained from H.C. Starck, Inc. are provided in Table 1. Glow discharge mass spectrometry (GDMS) results from Shiva Technology were generally within a factor of two of the chemical certification with the exception of oxygen, which may have resulted from the specimen preparation methods used for the GDMS analysis. The methods used to process the LCAC and TZM molybdenum have been described elsewhere [3,16,17,32]. Following wrought processing into sheet and plate, a final stress-relief anneal in vacuum was given at 850 °C/1 h for LCAC and 1150 °C/

Table 1
Chemical analysis of the LCAC sheet [3] and TZM plate (in weight ppm)

Material/lot#	C	O	N	Ti	Zr	Fe	Ni	Si	La	Al	Ca	Cr	Cu	Other
LCAC sheet, Ingot 40386A2, Heat# C18605, 0.51 mm sheet	90	3	4	NA	NA	10	<10	<10	NA	NA	NA	NA	NA	NA
LCAC Specification[a]	$\leqslant$100	$\leqslant$15	$\leqslant$20	NA	NA	$\leqslant$100	$\leqslant$20	$\leqslant$100	NA	NA	NA	NA	NA	NA
TZM plate, Ingot 61722B, Heat# TZM24080, 6.35 mm plate	223	17	9	5000	1140	<10	<10	<10	NA	NA	NA	NA	NA	NA
TZM specification[a]	100/300	$\leqslant$30	$\leqslant$20	4000/5500	600/1200	$\leqslant$100	$\leqslant$20	$\leqslant$100	NA	NA	NA	NA	NA	NA
GDMS data														
LCAC sheet	~100	~45	~2	8	0.95	20	2.2	1	<.005	1.7	0.1	3.9	0.3	150 W
TZM plate	280	90	7	5300	1400	12	1.3	3.5	0.02	0.91	<.05	2.8	0.2	210 W

NA = not available.
All material was obtained from H.C. Stark, which was formally known as CSM Industries, Inc., Cleveland, OH.
Trace GDMS composition for elements not listed was <1 ppm.
[a] ASTM B386 – 365 for arc-cast LCAC and B386 – 363 for TZM [9].

0.5 h for TZM. Previous work involved the use of recrystallized LCAC, but only stress-relieved material in the longitudinal stress-relieved (LSR) or transverse stress-relieved (TSR) condition was used in this work. The same sub-sized SS-1 flat tensile geometry [3] was used in this work with a nominal size of 44.45 mm long × 4.95 mm wide with a 20.32 × 1.52 mm gauge length and nominal thickness of either 0.76 mm or 0.40 mm. All tensile specimens were laser scribed for identification, electropolished, and then given a stress-relief anneal in vacuum at 850 °C for 1 h for LCAC and 1150 °C for 0.5 h for TZM [3,16].

A detailed description of the capsules used to irradiate the LCAC and TZM tensile specimens has been provided [3,31]. The individual capsules used for irradiation are identified in Table 2. Eight tensile specimens for each irradiation capsule were loaded into a rectangular axial opening machined into a 5.08 cm diameter × 5.6 cm long cylindrical specimen holder. Holders were made of aluminum for the 300 °C irradiation and vanadium for the 600 °C, and 1000 °C irradiations. The tensile holders were centered within the capsule using a thimble and then welded to seal an inert helium atmosphere inside each capsule. The irradiation temperatures were determined using a thermal model, and were primarily dependent on the size of gas-gaps between the holder/capsule. The maximum temperature difference through the thickness of the tensile specimens, as determined from thermal calculations, were 10 °C at an irradiation temperature of 300 °C and on the order of 25 °C at an irradiation temperature of 1000 °C. Thermal analysis calculations also indicated that the variation in irradiation temperature along the length of the tensile specimen was ±25 °C for the 600–1000 °C irradiations, and ±15 °C for the 300 °C irradiations. The irradiation temperatures were verified by using passive silicon carbide (SiC) temperature monitors [3,33]. Analysis of the temperature monitors shows in Table 2 that the irradiation temperatures were within 50 °C or less of the target irradiation temperatures for irradiations performed at 300 °C (determined to be 294 °C) and 600 °C (determined to be 560 °C), and within ±100 °C or less for irradiations at 1000 °C (determined to be 936 °C) [3].

All capsule irradiations were performed in the peripheral target tube position (PTP) of the High Flux Isotope Reactor (HFIR) in 3–10 cycles at 85 MW of

Table 2
Estimated irradiation temperature, neutron fluence, and calculated DPA values for LCAC and TZM molybdenum following irradiation in HFIR

Target irradiation temperature[a] (°C)	Actual specimen irradiation temperature[d] (°C)	Irradiation cycles[c]	Neutron fluence [$E > 0.1$ MeV], $\times 10^{24}$ n/m^2/(estimated molybdenum DPA)[b]: capsule ID			
LCAC molybdenum						
300	294	388–397	10.5/(0.6): b1	N/A	N/A	232/(12.3): f1/f2
600	560	388–397	16.2/(0.9): b2	27.0/(1.4): b5	N/A	246/(13.1): f4
600	784	388–397	N/A	N/A	N/A	246/(13.1): f3
1000	936	388–397	18.0/(1.0): b3	44.6/(2.4): b6	N/A	247/(13.1): f5/f6
1100	1100	N/A	22.9/(1.2): b4	44.7/(2.4): b7	61.3/(3.3): b9	N/A
TZM molybdenum						
300	294	388–397	N/A	N/A	N/A	232/(12.3): f1/f2
600	560	388–390/ 388–397	N/A	N/A	72.6/(3.9): n2	246/(13.1): f4
600	784	388–397	N/A	N/A	N/A	246/(13.1): f3
1000	936	388–390/ 388–397	N/A	N/A	73.3 (3.9): n4	247/(13.1): f5/f6

N/A indicates that irradiations were not performed at these conditions.

[a] The target irradiation temperature was the calculated tensile specimen temperature objective for the irradiation test. The irradiation temperatures were generally within ±50 °C for irradiations at 300 °C and 600 °C, and ±100 °C for irradiations performed at 1000 °C.

[b] The conversion from neutron fluence to molybdenum dpa for the HFIR spectrum was determined using the code SPECTER [36]. Note, previously reported fluence values (10.5–61.3 × 10^{24} n/m^2) for LCAC are shown in this table [3].

[c] Only irradiation cycles for the new work are reported. These irradiations were performed over a period of 26 July 2002 to 17 November 2003. Cycles 388, 389, and 390 were used to produce neutron fluences of 72.6–73.3 × 10^{24} n/m^2. The MW days and hours of operation for each cycle are as follows: cycle 388 (2094 MW days and 591.2 h), cycle 389 (2124 MW days and 599.7 h), cycle 390 (2111 MW days and 596.1 h), cycle 391 (2090 MW days and 590.0 h), cycle 392 (2077 MW days and 586.5 h), cycle 393 (2143 MW days and 605.0 h), cycle 394 (2130 MW days and 601.3 h), cycle 395 (2198 MW days and 620.6 h), cycle 396 (2203 MW days and 621.9 h), cycle 397 (2216 MW days and 625.8 h).

[d] Actual specimen irradiation temperatures determined from analysis of the temperature monitors. The irradiation temperatures are reported for the n2, n4, and f1 to f6 capsules. Results for the b1 to b9 capsules were previously reported [3,31].

power (see Table 2 for cycle designation and capsule designations). No effort was made to shield the capsules or specimens from the neutron spectrum that is produced by HFIR, which results in an estimated nominal peak fast neutron flux of 10×10^{18} n/m^2 s ($E > 0.1$ MeV), and a peak thermal neutron flux of 2.2×10^{19} n/m^2 s ($E < 0.1$ MeV). The displacement damage produced by the irradiation was primarily the result of the fast flux. Reactions resulting from thermal neutron absorption have been addressed in previous papers and are not thought to be a significant contribution to the irradiation damage [3,31]. Irradiation of molybdenum in HFIR to the maximum fluence values reported in Table 2 (3.9–12.4 dpa) is calculated to produce a very low concentration (<0.2 and 0.6 wt.%) of transmutation products that are primarily Tc and Ru with 3–4 ppm amounts of Zr and Nb [3,31,34]. Independent calculations of the transmutation products produced by irradiation using an ORIGEN-S point depletion computer program have confirmed the results reported by Greenwood and Garner [34]. Irradiation hardening is therefore expected to be the result of the agglomeration of point defects. Results in the following sections will show that the increase in tensile strength is saturated after a certain neutron fluence. Since the amount of transmutation products are increased at higher dose, these results suggest that the defects produced by irradiation have a dominant effect on the change in mechanical properties. Transmutation products are not believed to have a significant influence on the tensile results. However, further investigations are needed to clearly separate the role of irradiation produced defects and transmutation products on the change in mechanical properties.

Tensile testing was performed on non-irradiated and irradiated materials at temperatures ranging from −150 °C to 1000 °C at an actuator displacement rate of 0.017 mm/s (strain rate = 0.05 min^{-1}) in accordance with ASTM E8 [35]. Specimen load and crosshead displacement were monitored and used to determine the tensile properties in terms of engineering stress/strain. Room-temperature tests were conducted at atmospheric pressure, while elevated temperature tests were performed in a vacuum furnace ($< 6 \times 10^{-5}$ MPa) that was equipped with refractory-metal heating elements and heat shields. Heating to the test temperature was typically achieved in 30–45 min with a soak time of

Table 3
Summary of unirradiated tensile data for LCAC molybdenum sheet [3]

Test temperature (°C)	Tensile strength (MPa)		Tensile ductility (%)			Strain hardening exponent, n
	Ultimate tensile stress	0.2% Yield stress	Total elongation	Uniform elongation	Reduction in area	
Longitudinal stress-relieved						
−194	1410.0	1410.0	0	0	0	–
−150	1554.8	1554.8	<1	<1	0	–
−100	1210.8 ± 22.4	1251.1 ± 34.6[a,b,c]	9.2 ± 6.9	2.4 ± 2.3	26	0.027
−50	981.8 ± 14.6	995.6 ± 2.9[a,b,d]	16.8 ± 1.8	4.4 ± 4.3	44	0.038
0	801.2	832.2[a,b]	18	10	49	–
22	793.7 ± 6.2	751.9 ± 8.8	17.6 ± 1.5	7.7 ± 1.2	59 ± 4	0.044
150	646.7 ± 8.8	538.9 ± 13.2	9.8 ± 4.0	6.6 ± 3.7	62 ± 7	0.11
300	577.8 ± 10.7	505.4 ± 19.9	6.2 ± 0.8	3.5 ± 0.8	75	0.13
600	513.0 ± 13.5	475.6 ± 33.4	3.8 ± 0.5	1.5 ± 0.5	76 ± 3	0.11
700	501.3	464.0	4.4	1.8	70	0.078
800	443.0 ± 11.2	402.3 ± 23.9	5.7 ± 0.9	1.7 ± 0.5	95 ± 5	0.039
1000	311.0 ± 1.0	280.3 ± 24.9	6.3 ± 3.3	1.1 ± 0.1	98 ± 1	0.038
1093	136.5	110.3	23	–	98	–
Transverse stress-relieved						
−194	1753.4	1753.4	0	0	0	–
−150	1592.7	1592.7	<1	<1	0	–
−100	1307.3	1319.0[a,b]	9	<1	26	–
−50	1067.3	1073.6[a,b]	15	<1	37	–
22	824.6 ± 28.1	809.3 ± 19.7	13.1 ± 2.8	5.7 ± 0.5	45 ± 6	–
871	239.9	236.5	6	1	98	–

'–' means that a value was not measured for this condition.

[a] An upper/lower yield point is observed.

[b] A slight yield point is observed, resulting in a higher yield strength than the ultimate strength, or the yield strength being equivalent to the ultimate tensile strength.

[c] An upper yield point was observed with an upper yield point of 1275.6 MPa.

[d] An upper yield point was observed with an upper yield point of 993.6 MPa.

30 min prior to tensile testing. Tensile testing at sub-ambient temperatures was conducted in a controlled chamber using nitrogen gas cooling to achieve temperatures down to −150 °C [3]. Fractographic examinations were performed using scanning electron microscopy (SEM). Determination of the tensile DBTT was primarily based on the fracture mode.

3. Results and discussion

3.1. Unirradiated tensile properties

Tensile results for unirradiated LCAC and TZM molybdenum are summarized in Tables 3 and 4, respectively. The microstructures of TZM and LCAC are shown in Fig. 1 to consist of elongated, sheet-like pancaked grains with grain heights and lengths from the transverse and longitudinal orientation summarized in Table 5 [3]. LCAC has a low number density of coarse carbide inclusions. TZM contains a higher number density of coarse carbide precipitates. The grain dimensions were generally thinner and longer in the longitudinal orientation, which is consistent with the pancake shape of the grains. Slightly lower tensile strength and higher elongation values were observed in the longitudinal orientation for both LCAC and TZM molybdenum, and these non-isotropic tensile properties are consistent with literature data [3,9–17]. The presence of more grain boundary area in the TSR orientation provides a higher concentration of grain boundaries in the tensile orientation, which produce a higher tensile strength,

Table 4
Summary of unirradiated tensile data for TZM molybdenum

Test temperature (°C)	Tensile strength (MPa)		Tensile ductility (%)			Strain hardening exponent, *n*
	Ultimate tensile stress	0.2% Yield stress	Total elongation	Uniform elongation	Reduction in area	
Longitudinal stress-relieved						
−194	1445.0	N/A	0	0	0	–
−150	1435.9 ± 72.6	N/A	1 ± 1	0 ± 0	3	–
−100	1232.8 ± 25.5	1224.0 ± 33.2	1.9 ± 1.7	0.7 ± 0.1	7	–
−50	1030.5 ± 32.3	1019.7 ± 37.9	8.8 ± 7.3	4.2 ± 3.5	31 ± 12	0.031
0	854.3	803.3	19.6	8.5	–	–
RT	815.5 ± 31.0	740.1 ± 31.2	16.4 ± 2.9	8.9 ± 2.3	45 ± 8	0.076
100	755.7 ± 29.9	649.7 ± 18.8	12.3 ± 1.7	6.5 ± 1.3	65	0.13
200	673.9 ± 17.9	577.1 ± 12.3	9.0 ± 0.9	4.7 ± 1.5	61	–
300	698.1 ± 41.4	605.0 ± 7.3	8.1 ± 0.1	4.1 ± 3.0	58 ± 17	0.10
400	672.9	615.0	7.0	2.6	69	–
600	597.0 ± 34.3	546.5 ± 28.9	4.7 ± 0.2	2.4 ± 0.3	62	0.13
700	572.0 ± 21.5	525.2 ± 15.5	4.5 ± 0.4	2.0 ± 0.4	65 ± 15	0.12
800	551.1 ± 31.6	508.7 ± 23.0	4.2 ± 0.5	2.1 ± 0.3	61 ± 8	0.10
976	487	448	5.0	1.6	>99	–
1000	518.1 ± 19.6	482.9 ± 21.4	3.7 ± 0.5	1.5 ± 0.3	67	0.045
1201	414.4	401.9	7.0	7.0	86	–
1406	172.4	106.9	30	30	97	–
Transverse stress-relieved						
−194	1390.0	N/A	0	0	0	–
−150	1535.5	N/A	<1	<1	0	–
−100	1333.6 ± 14.4	1328.0 ± 22.4	0.8 ± 0.2	0.6 ± 0.0	0	–
−50	1154.7 ± 61.1	1169.9 ± 55.9	4.3 ± 2.9	0.6 ± 0.1	13	–
0	928.8	895.0	11.0	6.0	40	–
RT	851.7 ± 27.0	810.0 ± 43.8	11.7 ± 1.7	5.4 ± 0.5	36	–
100	814.5 ± 17.7	761.0 ± 22.7	8.6 ± 2.2	4.2 ± 1.1	47	–
200	720.8 ± 27.4	662.4 ± 38.0	6.3 ± 1.1	3.5 ± 0.6	55	–
300	693.6	651.6	5.0	3.0	61	–
400	648.1	606.8	6.0	2.0	68	–
600	669.8 ± 20.0	637.4 ± 9.3	2.5 ± 0.4	1.0 ± 0.1	54	–
701	602.9 ± 11.2	558.5 ± 20.5	3.5 ± 0.8	0.9 ± 0.1	57 ± 4	–
800	593.0 ± 23.9	569.0 ± 24.1	2.7 ± 0.4	0.9 ± 0.1	–	–
1000	570.4 ± 35.3	550.4 ± 33.6	2.6 ± 0.4	0.9 ± 0.1	–	–

'–' means that a value was not measured for this condition.
Some results were previously reported [17].

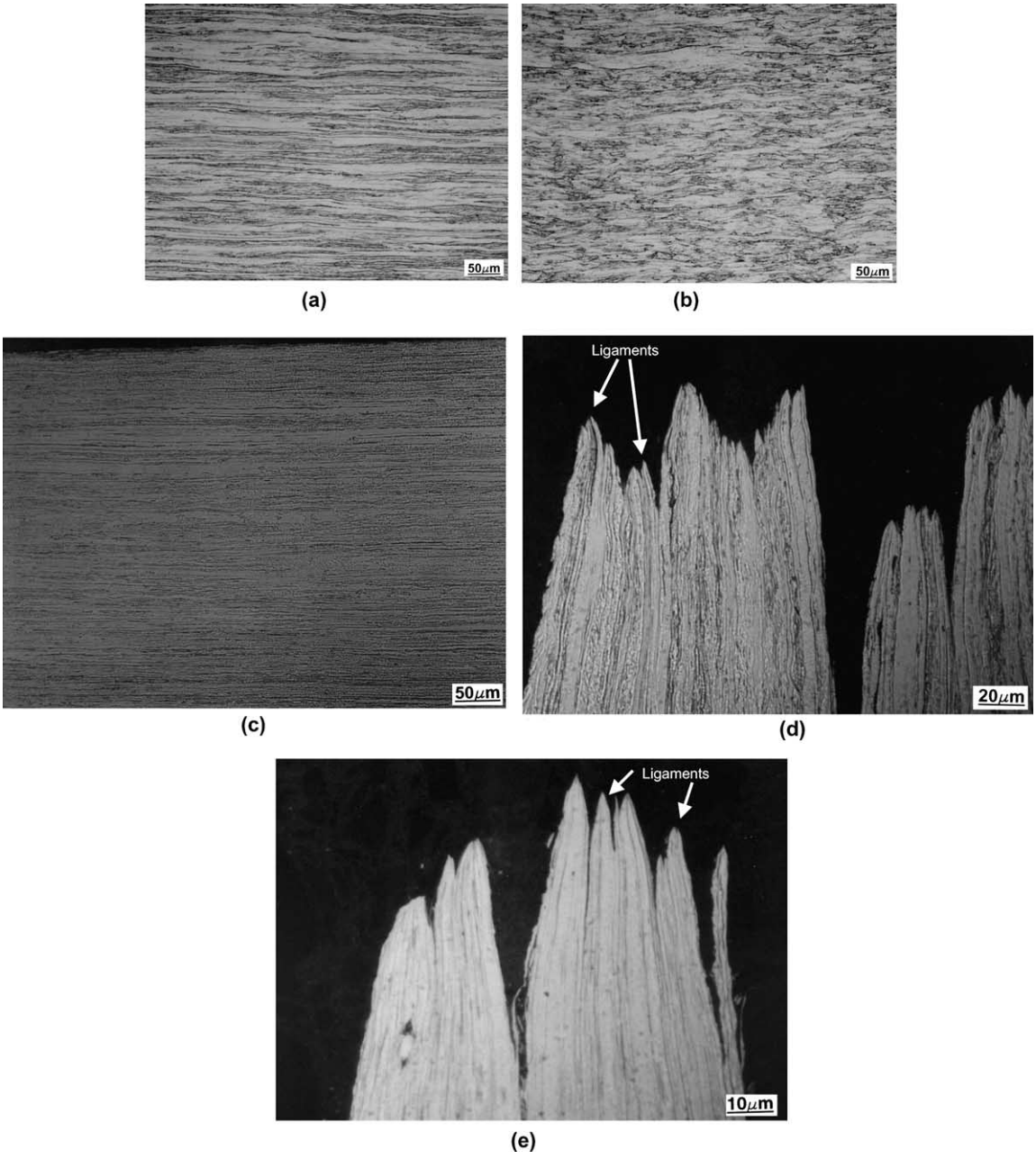

Fig. 1. Optical micrographs of molybdenum alloy tensile specimens: (a) TZM molybdenum in the longitudinal orientation, (b) TZM molybdenum in the transverse orientation, (c) LCAC molybdenum in the longitudinal orientation, (d) TZM molybdenum tested at room temperature near the fracture surface showing a ductile-laminate failure, and (e) LCAC tested at room temperature, near the fracture surface showing a ductile-laminate failure mode.

but fracture initiation generally occurs at grain boundaries, which results in a lower tensile elongation for the TSR orientations. Although the greater amount of work used to form the LCAC sheet results in a slightly finer grain size, which would be expected to result in a higher tensile strength in accordance with Hall–Petch grain boundary strengthening, the solid solution strengthening and coarse carbide precipitates present in TZM result in slightly higher tensile strength values than found in LCAC. Additionally, TZM is more resistant to recrystallization and recovery than LCAC molybdenum, which results in significantly higher

Table 5
Summary of grain size measurements for LCAC sheet and TZM plate

Alloy	Grain diameter (μm)		Grain length (μm)	
	Average	Standard deviation	Average	Standard deviation
LCAC sheet – LSR	3.9	2.5	172	79
LCAC sheet – TSR	5.0	2.7	78.1	38.2
TZM plate – LSR	3.9	2.5	273	105
TZM plate – TSR	6.1	3.8	132	69

strength at test temperatures ⩾800 °C. LCAC has been shown to start and complete recrystallization at 1000 °C and 1100 °C for 1 h heat treatments, which explains the lower tensile strength at temperatures ⩾ 800 °C.

Load–displacement curves for LCAC and TZM molybdenum, which have not been corrected for the compliance of the load train, show in Fig. 2 that a low work hardening rate, with strain hardening exponents ranging from 0.027 to 0.13 (Tables 3 and 4), is observed that is consistent with the literature data [3,10–14,19–29]. The fracture surfaces for both LCAC and TZM are shown in Fig. 3 to consist of a ductile-laminate failure, where fracture initiation occurs at grain boundaries in the region of triaxial stresses to produce separation of

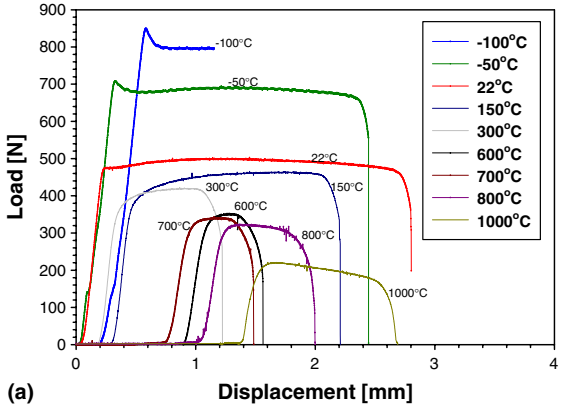

Test Temp	-100°C	-50°C	22°C	150°C	300°C	600°C	700°C	800°C	1000°C
n	0.027	0.038	0.044	0.11	0.13	0.11	0.078	0.039	0.038

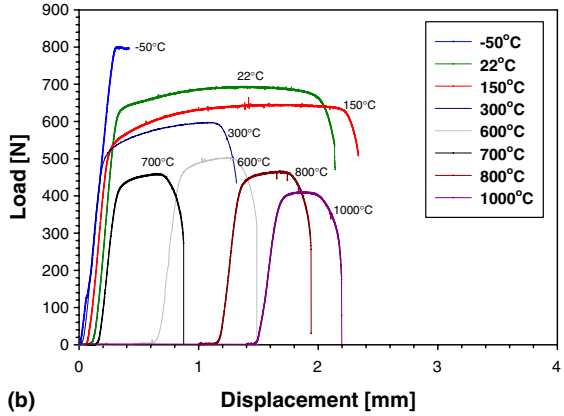

Test Temp	-50°C	22°C	150°C	300°C	600°C	700°C	800°C	1000°C
n	0.031	0.076	0.13	0.10	0.13	0.12	0.10	0.045

Fig. 2. Load–displacement curves for non-irradiated alloys in the LSR orientation: (a) LCAC molybdenum and (b) TZM molybdenum. Values for the strain hardening exponents are given, and are summarized in Tables 3 and 4.

the microstructure into laminate type grains that are then pulled to fracture with a high degree of necking [3,16,17]. Cross-sections of the tensile specimens near the fracture surfaces show in Fig. 1(d) and (e) the splitting of the grains into laminates at the fracture surface to produce the ductile-laminate failure mode. This fracture mechanism is also known as thin sheet toughening [37,38]. The ductile-laminate failure mode together with large values of total elongation and Reduction in Area (RA) were observed for LCAC and TZM molybdenum at temperatures equal to or greater than −100 °C and −50 °C, respectively. Low ductility and a brittle failure mode of transgranular cleavage were observed for LCAC molybdenum at or below −150 °C and TZM molybdenum at or below −100 °C. The transition from high amounts of ductility and ductile failure mode to low ductility and brittle failure mode was observed at the same respective temperatures for both the longitudinal and transverse orientations of LCAC and TZM. These results indicate that the tensile DBTT was between −150 °C and −100 °C for LCAC and between −100 °C and −50 °C for TZM (see Table 6).

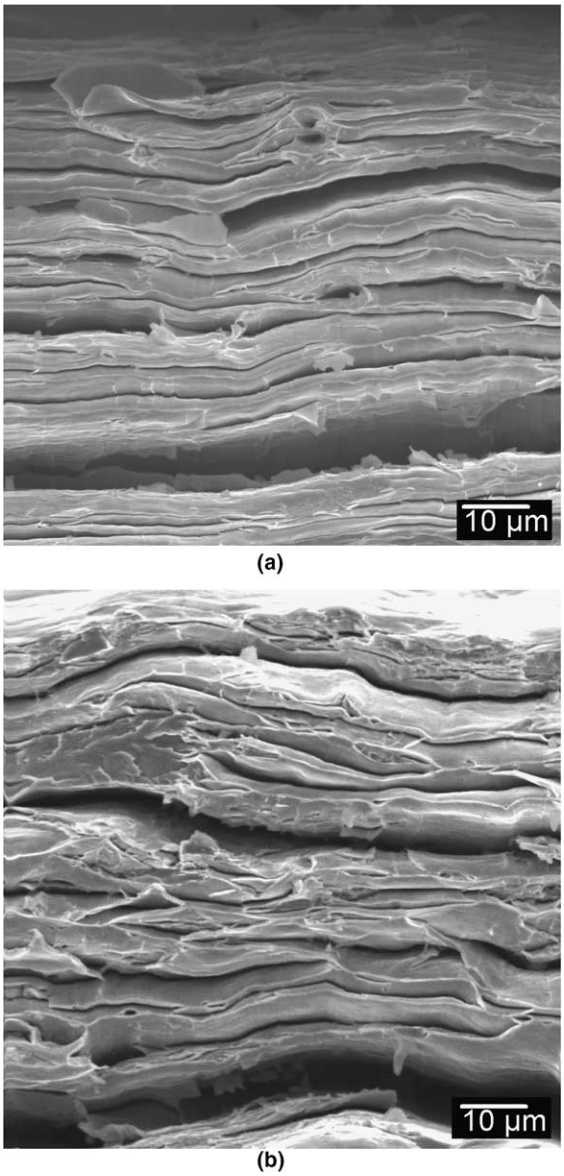

Fig. 3. SEM fractography of non-irradiated LCAC and TZM molybdenum following tensile testing at room temperature: (a) LCAC molybdenum and (b) TZM molybdenum.

3.2. Post-irradiation tensile properties for irradiation at 300 °C and 600 °C

Post-irradiation tensile data obtained for LCAC and TZM molybdenum are provided in Tables 7 and 8, respectively. The true specimen irradiation temperatures are provided in Tables 2,7, and 8, which are 294 °C and 560 °C, but all references to irradiation temperature in the following discussions are made with respect to the target irradiation temperatures of 300 °C and 600 °C. Large increases in yield strength and large amounts of irradiation hardening, which is reflected by the increase in yield strength, are observed for the irradiation of LCAC and TZM molybdenum at 300 °C and 600 °C in Figs. 4 and 5, respectively, with percent increases ranging from 23% to 174%, which is consistent with literature data [1–8,18–28]. The irradiation hardening values observed for LCAC and TZM molybdenum are generally comparable at all test and irradiation temperatures. The hardening results for irradiations performed at 300 °C and 600 °C are also quite similar. It should be noted that the tensile strength values determined at temperatures <DBTT actually reflect the fracture stress. In the brittle regime the material fractures before yielding. Scatter in the size and distribution of pre-existing flaws results in the scatter of the fracture strength values determined for LCAC and TZM molybdenum. Within the data scatter, the fracture stress values are independent of test temperature at temperatures below the DBTT.

The one exception to the similarity in irradiation hardening results for the 300 °C and 600 °C irradiations is that exceptionally low tensile strength and high levels of ductility were observed for one capsule (f3) that was intended to be irradiated at 600 °C, but analysis of the temperature monitors indicated that the nominal irradiation temperature was close to 754 °C (see Table 2). All specimens from capsule f3 exhibited tensile properties and change in electrical resistivity results that were comparable to specimens that were irradiated at 1000 °C. Analysis of temperature monitors confirmed that the last irradiation temperature for capsule f3 was 784 °C, which is well above 600 °C. This indicates that the temperature of irradiation for capsule f3 was inadvertently

Table 6
Summary of pre- and post-irradiation DBTT values determined from tensile testing for LCAC and TZM molybdenum following irradiation in HFIR to a maximum fluence of $2.32–2.47 \times 10^{26}$ n/m^2, $E > 0.1$ MeV

Alloy/condition	Pre-irradiation DBTT (°C)	Post-irradiated DBTT for irradiation at various irradiation temperatures (°C)		
		294	560/605	870–1100
LCAC – LSR	−100	800	300	−50
LCAC – TSR	−100	N/A	N/A	<25
TZM – LSR	−50	800	700	−50
TZM – TSR	−50	N/A	700	<0

For pre-irradiation DBTT values, the result is based on a ductile failure observed at −100 °C with a brittle failure observed at −150 °C. Post-irradiated DBTT values for 294 °C irradiations (800 °C) are based on a ductile failure observed at 800 °C with a brittle failure observed at 700 °C. For 560 °C irradiations, the 300 °C DBTT for LCAC is based on a ductile failure observed at 300 °C and brittle failure observed at 150 °C, while the 700 °C DBTT for TZM is based on a ductile failure observed at 700 °C with a brittle failure observed at 600 °C. For 936 °C irradiations, the −50 °C DBTT is based on a ductile failure observed at −50 °C with a brittle failure mode observed at a temperature of −100 °C.

Table 7
Summary of irradiated tensile data for LSR LCAC molybdenum sheet

Irradiation temperature (°C)/capsule	Neutron fluence (n/m^2) ($E > 0.1$ MeV)	Test temperature (°C)	Tensile strength (MPa)		Tensile ductility (%)			Strain hardening exponent, n
			Ultimate tensile stress	0.2% Yield stress	Total elongation	Uniform elongation	Reduction in area	
294/f2	232×10^{24}	22	1244.5	1244.5[a,c]	0.06	0.06	0	–
294/f1	232×10^{24}	600	1190.8	1190.8[a]	0.03	0.03	1	–
294/f2	232×10^{24}	700	944.6	944.6[a]	0.11	0.11	2	–
294/f1	232×10^{24}	800	637.8	638.5[b]	1.8	0.2	64	−3.10
560/f4	246×10^{24}	22	1386.6	1386.6[a]	0.03	0.03	0	–
560/f4	246×10^{24}	150	1475.5	1475.5[a]	0.05	0.05	0	–
784/f3[d]	246×10^{24}	300	630.9	559.9	2.7	1.0	66	0.40
784/f3[d]	246×10^{24}	600	508.9	463.3	2.5	0.7	77	0.36
936/f5	247×10^{24}	−100	1212.8	1212.8[b,e]	0.3	0.1	1	–
936/f6	247×10^{24}	−50	1024.6	1024.6[b,f]	1.5	0.05	20	−0.058
936/f5	247×10^{24}	22	687.4	692.3[b]	6.3	1.3	62	−0.012
936/f6	247×10^{24}	1000	376.5	399.9	4.1	2.0	63	0.090

'–' means that reduction in area was not measured for this condition.
[a] Since the uniform elongation was <0.2%, the yield strength cannot be determined, and is listed as being equal to the ultimate strength.
[b] A slight yield point is observed, resulting in a higher yield strength than the ultimate strength, or the yield strength being equivalent to the ultimate tensile strength.
[c] Initial fracture at pinhole followed by a second test shoulder loading.
[d] The irradiation temperature for these specimens exceeded 600 °C by a large margin at some point during the irradiation.
[e] An upper/lower yield point was observed with values of 1212.8/1136.3 MPa.
[f] An upper/lower yield point was observed with values of 1024.6/950.1 MPa.

well above 600 °C (possibly as high as 1000 °C with temperature monitor data indicating a nominal temperature of 784 °C) for a significant period of time during the irradiations. Assuming the irradiation of capsule f3 actually occurred for some period of time at 600 °C, and was followed by an increase in the nominal irradiation temperature to 784 °C for some period of time, these results suggest that irradiation at high temperatures results in the recovery of the defect structures that produce irradiation embrittlement. Tensile results, change in electrical resistivity from the specimens, and analysis of the temperature monitors in capsule f4 were consistent with the lower fluence results for 560 °C irradiations, which indicates that the capsule f4 specimens were irradiated at 560 °C. Further discussion of results from the f3 capsule will not be pursued, but these results

Table 8
Summary of irradiated tensile data for TZM molybdenum plate

Irradiation temperature (°C)/capsule	Neutron fluence (n/m^2) ($E > 0.1$ MeV)	Test temperature (°C)	Tensile strength (MPa)		Tensile ductility (%)			Strain hardening exponent, n
			Ultimate tensile stress	0.2% Yield stress	Total elongation	Uniform elongation	Reduction in area	
Longitudinal stress-relieved								
294/f2	232×10^{24}	22	912.9	912.9[a,c]	0.01	0.01	0	–
294/f1	232×10^{24}	600	1166.6	1166.6[a]	0.01	0.01	0	–
294/f2	232×10^{24}	700	1094.9	1094.9[a]	0.09	0.09	1	–
294/f1	232×10^{24}	800	920.5	920.5[b]	1.7	0.2	66	−4.06
560/n2	72.6×10^{24}	22	1339.0	1339.0[a]	0.0	0.0	0	–
560/n2	72.6×10^{24}	22	927.4	927.4[a]	0.0	0.0	–	–
560/n2	72.6×10^{24}	600	1305.2	1305.2[a]	0.41	0.16	0	–
560/n2	72.6×10^{24}	600	1280.4	1280.4[a]	0.07	0.07	–	–
560/n2	72.6×10^{24}	700	1206.6	1208.0[b]	0.33	0.21	3	−0.18
560/n2	72.6×10^{24}	800	1032.9	1030.1	0.47	0.27	6	0.14
560/f4	246×10^{24}	300	899.8	899.8[a,c]	0.00	0.00	0	–
784/f3[d]	246×10^{24}	600	941.2	921.2	1.9	0.4	48	0.47
784/f3[d]	246×10^{24}	700	761.2	739.1	2.1	0.5	60	0.66
936/n4	73.3×10^{24}	−50	1198.4	1198.4[a]	0.68	0.11	0	−0.21
936/n4	73.3×10^{24}	0	1092.2	1092.2[a]	0.73	0.04	–	0.08
936/n4	73.3×10^{24}	22	969.4	982.5[b]	0.87	0.84	2	–
936/n4	73.3×10^{24}	22	963.9	927.4	7.82	5.24	–	0.037
936/n4	73.3×10^{24}	1000	639.9	627.4	2.79	0.63	–	–
936/n4	73.3×10^{24}	1000	623.3	610.9	2.79	0.80	–	0.036
936/f6	247×10^{24}	−100	1391.4	1391.4[b,e]	3.2	0.05	32	−0.13
936/f5	247×10^{24}	−50	1155.6	1155.6[b,f]	5.3	0.04	45	−0.11
936/f5	247×10^{24}	23	899.8	882.6	7.1	4.0	44	0.018
936/f6	247×10^{24}	1000	593.0	588.1	3.9	0.7	–	0.042
Transverse stress-relieved								
560/n2	72.6×10^{24}	700	1230.1	1231.4[a]	0.50	0.30	1	–
560/n2	72.6×10^{24}	800	1051.5	1048.7	1.20	0.32	6	–
936/n4	73.3×10^{24}	0	1002.5	1031.5[b]	6.24	3.25	–	–
936/n4	73.3×10^{24}	22	966.7	980.5[b]	6.33	3.46	–	–

'–' means that reduction in area was not measured for this condition.
[a] Since the uniform elongation was <0.2%, the yield strength cannot be determined, and is listed as being equal to the ultimate strength.
[b] A slight yield point is observed, resulting in a higher yield strength than the ultimate strength, or the yield strength being equivalent to the ultimate tensile strength.
[c] Initial fracture at pinhole followed by a second test shoulder loading.
[d] The irradiation temperature for these specimens exceeded 600 °C by a large margin at some point during the irradiation.
[e] An upper/lower yield point was observed with values of 1391.4/1327.3 MPa.
[f] An upper/lower yield point was observed with values of 1155.6/1057.0 MPa.

indicate that irradiation of molybdenum at a nominal temperature of 784 °C does not result in irradiation embrittlement.

For irradiations at 300 °C, the irradiation hardening and tensile strength values determined for LCAC and TZM molybdenum at a fluence of 2.32×10^{26} n/m^2 were comparable, and were also similar to lower dose (1.05×10^{25} n/m^2) results for LCAC [3]. This suggests that saturation of the irradiation defects is produced during 300 °C irradiations by a neutron fluence of 1.05×10^{25} n/m^2 or less. For irradiations at 600 °C, the post-irradiated tensile and irradiation hardening results determined for TZM at a fluence of 2.46×10^{26} n/m^2 and 7.26×10^{25} n/m^2 are considered to be comparable, while the tensile strength results for LCAC determined at a fluence of 2.46×10^{26} n/m^2 are slightly higher than previously determined at a fluence between 1.60 and 2.70×10^{25} n/m^2 [3]. This indicates that saturation in irradiation hardening for the 600 °C irradiations occurs at a fluence between 2.70 and 7.26×10^{25} n/m^2. The minimum fluence needed for saturation of irradiation strengthening for the 600 °C irradiations (7.26×10^{25}

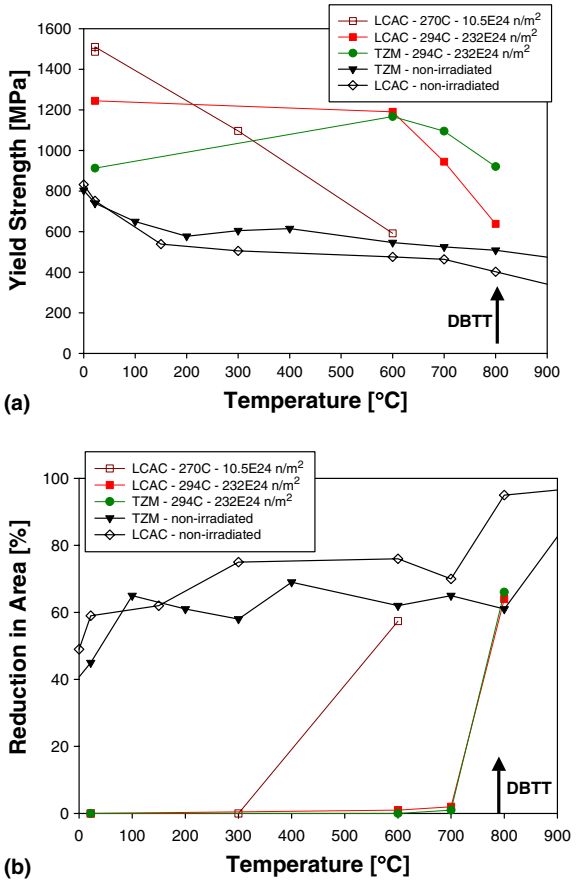

Fig. 4. Comparison of non-irradiated and post-irradiated tensile properties for LCAC and TZM molybdenum following irradiation at the target temperature of 300 °C (actual temperature of 294 °C): (a) yield strength values and (b) reduction in area values. Some results previously reported for LCAC are shown [3]. The tensile strength values determined at temperatures below the DBTT are actually a fracture stress in some cases as true plastic deformation has not been achieved.

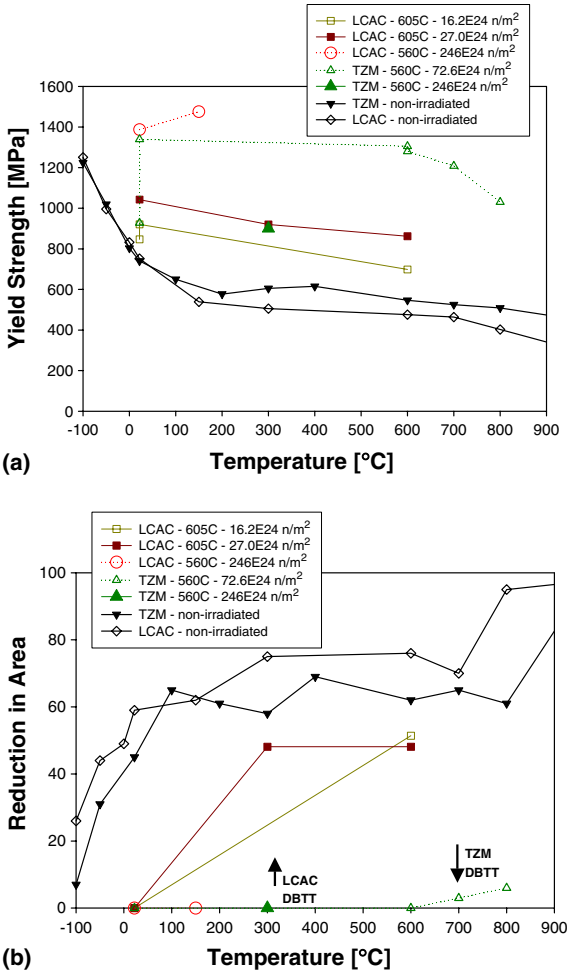

Fig. 5. Comparison of non-irradiated and post-irradiated tensile properties for LCAC and TZM molybdenum for irradiations at the target temperature of 600 °C (actual temperature of 560 °C) with some previous results [3]: (a) yield strength values and (b) reduction in area values. The tensile strength values determined at temperatures below the DBTT are actually a fracture stress in some cases as true plastic deformation has not been achieved.

n/m^2) is much higher than that needed for the 300 °C irradiations (1.05×10^{25} n/m^2), which indicates that a stable distribution of obstacles forms much more quickly for the 300 °C irradiations. A higher number density of fine loops and voids are expected to be formed by the 300 °C irradiations [1,4,5,8,18–22] that can form a stable distribution of obstacles more quickly than the larger voids that are expected to be formed during the 600 °C irradiations. Although the distributions of defects that would be expected to form during irradiations at 300 °C (high number density of fine loops and voids) and 600 °C (lower number density of coarser voids) are very different, the irradiated tensile strength values determined at saturation are similar, which are a fracture strength. This indicates that the spacing and number density of defects formed by irradiations of LCAC and TZM at 300–600 °C to saturation are such that dislocation mobility is equally inhibited for both conditions, and the true yield stress is elevated to a level well above the effective fracture stress of the material so that the tensile stress values being measured are actually a fracture stress. Since fracture stress is a function of pre-existing flaw sizes and inherent toughness of the material, comparable fracture stress values would be expected when plastic flow is equally limited, which is apparently the case for 300 °C and 600 °C irradiations at saturation.

Both LCAC and TZM molybdenum irradiated at 300 °C exhibit low amounts of tensile ductility and linear-elastic behavior to failure in the load–displacement

curves (Fig. 6) at test temperatures between room temperature and 700 °C. A brittle failure mode consisting of transgranular cleavage was observed for both alloys at room temperature, while a mixed-mode failure consisting primarily of transgranular cleavage with local regions of ductile-laminate failure was observed at 600 °C and 700 °C, see Fig. 7(a) and (b). Measurable tensile ductility, plasticity in the load–displacement curves, and a ductile failure mode (Fig. 7(c) and (d)) were observed for 300 °C irradiated LCAC and TZM molybdenum at a test temperature of 800 °C, which indicates that the tensile DBTT was no more than 800 °C (Table 6). Comparisons with previous results for LCAC irradiated to a lower fluence of 1.05×10^{25} n/m^2 [3] show an increase in DBTT from 600 °C to 800 °C results from irradiation to a higher dose of 2.32×10^{26} n/m^2. Although saturation of the increase in tensile strength for 300 °C irradiations occurs at a neutron fluence of

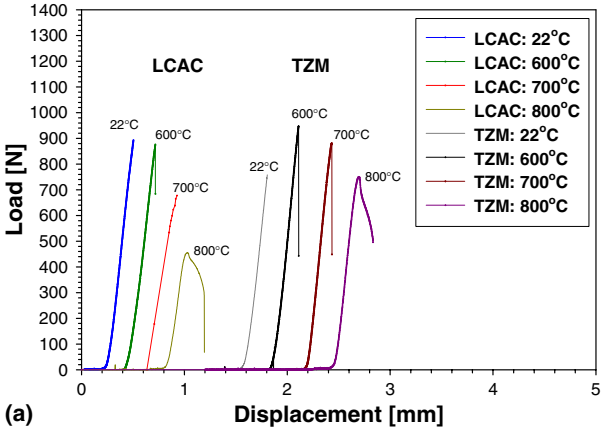

Alloy	LCAC				TZM			
Test Temp	22°C	600°C	700°C	800°C	22°C	600°C	700°C	800°C
n	--	--	--	-3.10	--	--	--	-4.06

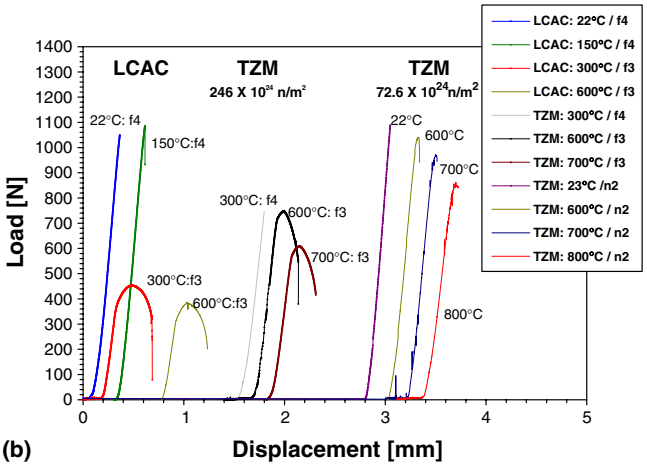

Alloy	LCAC				TZM						
Capsule	f4	f4	f3	f3	f4	f3	f3	n2	n2	n2	n2
Test Temp	22°C	150°C	300°C	600°C	300°C	600°C	700°C	22°C	600°C	700°C	800°C
n	--	--	0.40	0.36	--	0.47	0.66	--	--	-0.18	0.14

Fig. 6. Plot of load–displacement curves for LCAC and TZM molybdenum in the LSR orientation tested a temperatures between room temperature and 800 °C following irradiation at (a) 294 °C and (b) 560 °C. For the case of the 600 °C target irradiations to a fluence of 246×10^{24} n/m^2, the capsule is noted as either f4 (560 °C irradiation temperature) or f3 (irradiation temperature of 784 °C). For TZM, capsule n2 irradiations at 560 °C had a dose of 72.6×10^{24} n/m^2. Values for the strain hardening exponents are given with a summary of these values provided in Tables 7 and 8.

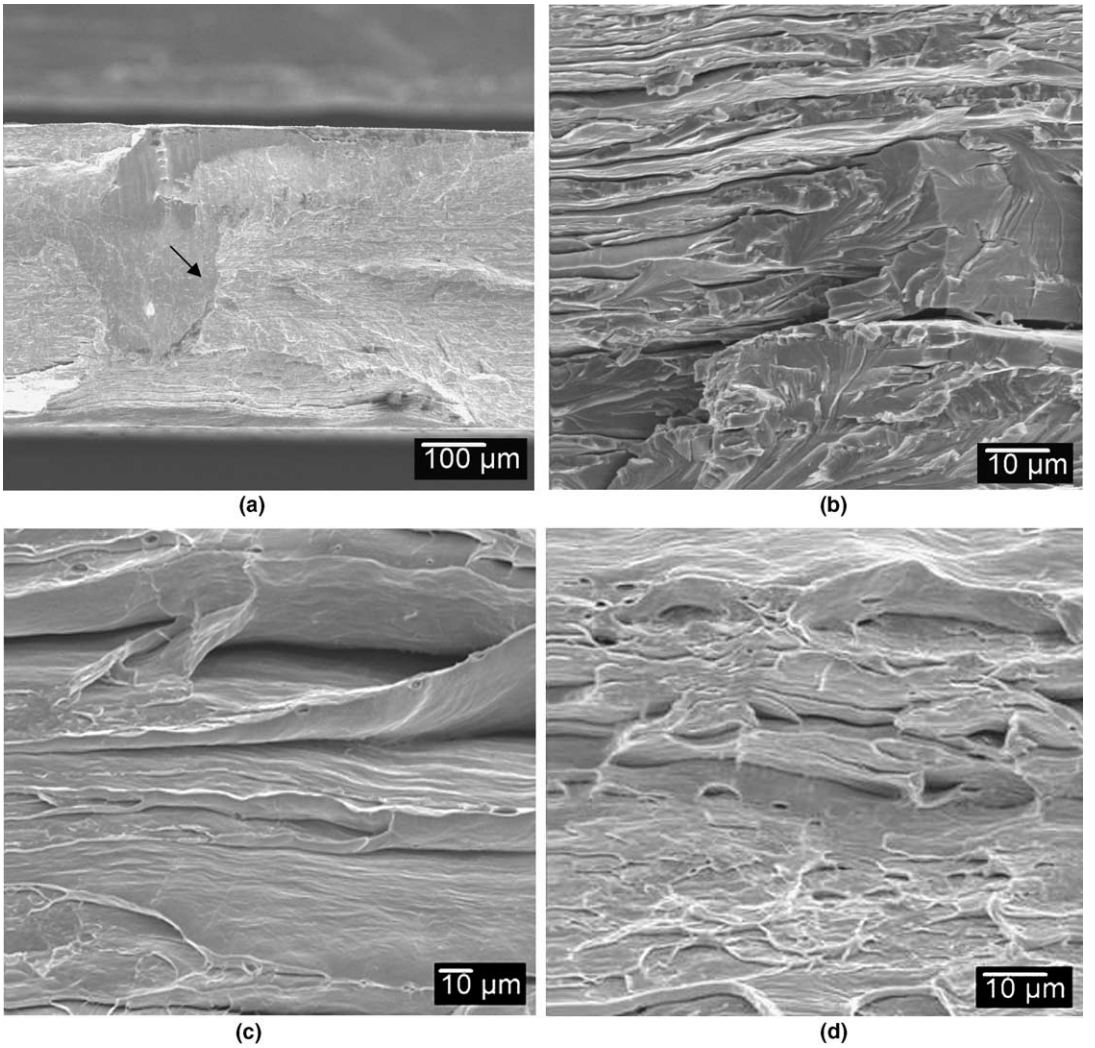

Fig. 7. Post-irradiated SEM fractography of TZM and LCAC molybdenum following 294 °C irradiations to 2.32×10^{26} n/m^2 for tensile testing of (a) LCAC tested at room temperature with the fracture initiation site indicated, (b) TZM tested at 600 °C, (c) LCAC tested at 800 °C, and (d) TZM tested at 800 °C.

1.05×10^{25} n/m^2, these results show that an increase in DBTT is observed at higher dose. This indicates that further changes in the defect structure are occurring with higher dose that have an effect on defect recovery and temperatures at which climb/glide mechanisms can be initiated to produce plasticity. However, the presence of mixed-mode failures with ductile-laminate features at 600 °C and 700 °C where no tensile ductility was measured indicates that higher amounts of energy may be absorbed during fracture, which could be resolved using fracture toughness testing.

The tensile DBTT for LSR LCAC irradiated at 600 °C to fluences of 1.62×10^{25} n/m^2 and 2.70×10^{25} n/m^2 was previously determined to be 300 °C, which is based on ductile tensile behavior being observed at 300 °C with brittle failure observed at room temperature [3]. Low tensile ductility, linear-elastic behavior with no plasticity in the load–displacement curves, and a brittle failure mode consisting of transgranular cleavage (Fig. 8(a)) were observed for LSR LCAC irradiated at 600 °C to a higher dose of 2.46×10^{26} n/m^2 after tensile testing at room temperature and 150 °C. These results are consistent with the DBTT of 300 °C that was previously determined for 600 °C irradiated LSR LCAC irradiated to a lower dose ($1.62–2.70 \times 10^{25}$ n/m^2), but these results cannot be used to determine the DBTT of LSR LCAC irradiated at 600 °C to the higher dose of 2.46×10^{26} n/m^2. Since saturation of the increase in the DBTT of 600 °C irradiated LSR LCAC was observed to occur at a fluence of 1.62×10^{25} n/m^2 [3],

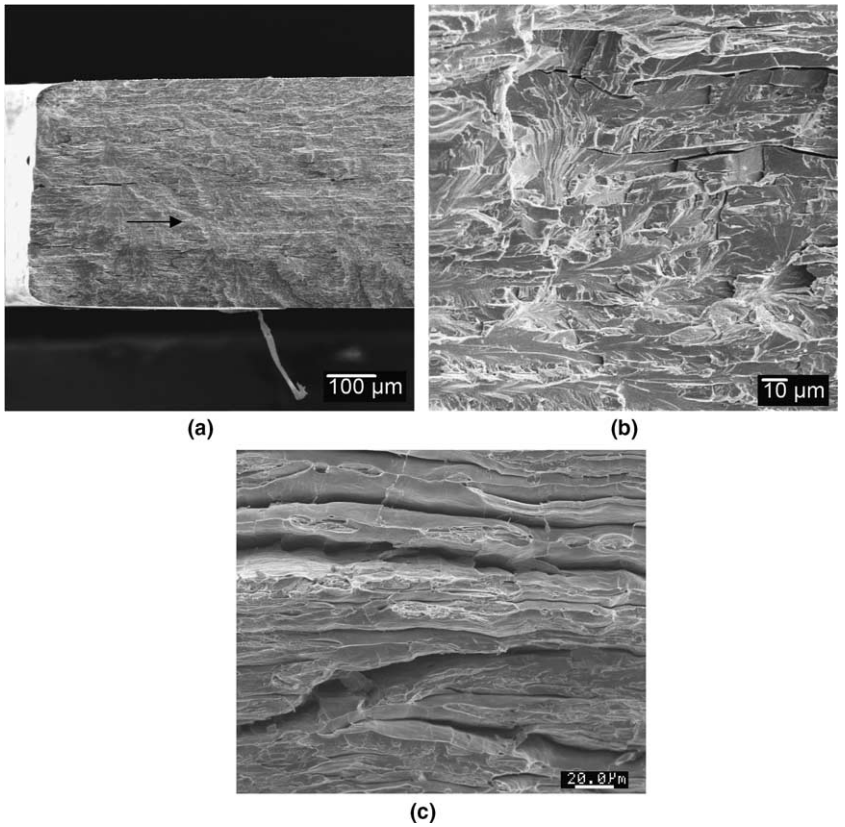

Fig. 8. Post-irradiated SEM fractography of TZM and LCAC molybdenum after irradiations at 560 °C for tensile testing of (a) LCAC tested at 150 °C with the fracture initiation site indicated, (b) TZM tested at 300 °C, and (c) TZM tested at 700 °C from a neutron fluence of 7.26×10^{25} n/m^2. With the exception of (c), all specimens were at a fluence of 2.46×10^{26} n/m^2.

the DBTT of 600 °C irradiated LSR LCAC could be expected to also be 300 °C following exposure to the higher dose of 2.46×10^{26} n/m^2. Irradiation of TZM at 600 °C to a lower dose of 7.26×10^{25} n/m^2 was shown to result in low ductility, linear-elastic behavior in the load–displacement curves, and a brittle failure mode of transgranular cleavage (Fig. 8(b)) for tensile testing at room temperature to 600 °C. Some tensile ductility was measured at 700 °C with slight plasticity observed in the load–displacement curve, and a ductile failure mode consisting of ductile-laminate features (Fig. 8(c)), which indicates that the DBTT for 600 °C irradiated TZM was 700 °C for both the longitudinal and transverse orientations. The low ductility and brittle failure mode observed for TZM irradiated at 600 °C to a higher dose of 2.46×10^{26} n/m^2 at a test temperature of 300 °C is consistent with the 700 °C DBTT that was determined at a lower dose. Since saturation of the DBTT for 600 °C irradiated LCAC was previously shown to occur at a dose of 1.62×10^{25} n/m^2, the DBTT for 600 °C irradiated TZM would be expected to be saturated after exposure to a dose of 7.26×10^{25} n/m^2, which indicates

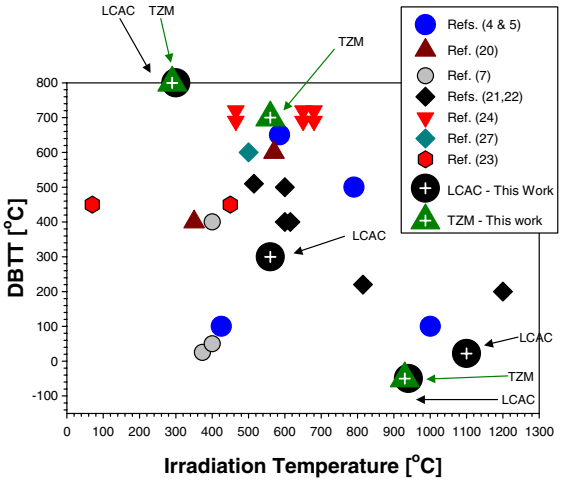

Fig. 9. Summary of results for LCAC and TZM DBTT values obtained in this work compared with literature data for molybdenum as a function of irradiation temperature. A summary of the DBTT values and fluences for the literature data summarized here is provided in Table 9.

that the DBTT of TZM likely remains at 700 °C after the 600 °C irradiation to a dose of 2.46×10^{26} n/m^2, see Table 6.

The brittle failure mode that were observed for LCAC and TZM irradiated at 300 °C and 600 °C and then tested at temperatures below the DBTT was always transgranular cleavage, which indicates that grain boundaries of these molybdenum alloys were not embrittled by irradiation to the point of being a preferred fracture path. Fracture initiation sites were observed to be small linear defects that could be either a microcrack or grain boundary, but further investigations are needed to identify the initiation site. The failure mode and initiation sites did not change with irradiation dose [3]. All failures at test temperature above the DBTT were observed to occur by the same ductile-laminate failure mode that was observed for non-irradiated material.

Comparison with the DBTT values reported in the literature for irradiated molybdenum show (Fig. 9) that the DBTT values obtained for the 300 °C irradiations were higher than literature data at a similar irradiation temperature, which is probably explained by the significantly lower dose for the literature data compared to the dose used in this work. The literature data plotted in Fig. 9 are summarized in Table 9 with the reported dose values. This observation supports the results observed in this work for the 300 °C irradiations where saturation of the increase in DBTT was not observed at the low fluence values of 1.05×10^{25} n/m^2. The DBTT for 600 °C irradiated LCAC molybdenum (300 °C) is shown in Fig. 9 to be at the lower end of the range of DBTT values (100–700 °C) reported in the literature when high dose irradiations are considered, while the 700 °C DBTT determined for TZM is consistent with 600 °C literature data for irradiations close to the dose used in this work. These results indicate that the LCAC molybdenum evaluated in this work exhibits some limited resistance to radiation embrittlement for 600 °C irradiations [3] relative to TZM and other molybdenum alloys irradiated to high dose where the DBTT is close to 700 °C, but

Table 9
Summary of irradiation temperature, DBTT, and neutron fluences for the literature data plotted in Fig. 9, and data reported in this study from Table 6

Irradiation temperature (°C)	Neutron fluence (n/m^2) ($E > 0.1$ MeV)	DBTT (°C)	References
70	3.5×10^{24}	450	[23]
450	2.9×10^{24}	450	
500	100×10^{24}	600	[27]
465	140×10^{24}	720	[24]
650	190×10^{24}	720	
680	190×10^{24}	720	
465	140×10^{24}	690	
650	190×10^{24}	690	
680	190×10^{24}	690	
515	12×10^{24}	510	[21,22]
615	12×10^{24}	400	
815	12×10^{24}	220	
600	12×10^{24}	400	
1200	27×10^{24}	200	
373	197×10^{24}	25	[7]
400	946×10^{24}	400	
400	946×10^{24}	50	
350	40×10^{24}	400	[20]
570	57×10^{24}	600	
425	250×10^{24}	100	[4,5]
585	250×10^{24}	650	
790	250×10^{24}	500	
1000	440×10^{24}	100	
LCAC molybdenum			
294	232×10^{24}	800	This work
560	246×10^{24}	300	
936	247×10^{24}	−50	
TZM molybdenum			
294	232×10^{24}	800	This work
560	246×10^{24}	700	
936	247×10^{24}	−50	

both LCAC and TZM are equally embrittled by irradiations at 300 °C. One exception for the literature data is discussed in the following paragraph.

The use of arc-cast processing results in a low oxygen and relatively low carbon content, and the wrought microstructure with fine, elongated pancaked grains may result in better resistance to irradiation embrittlement. Literature data has indicated that wrought molybdenum with a fine grained, elongated sheet-like grain structure, and much lower carbon content than for the LCAC used here has a DBTT of room temperature after irradiations at 373 °C, 519 °C, and 600 °C to neutron fluences between 1.97 and 9.46×10^{26} n/m^2 [7]. This provides additional evidence that a fine-grained microstructure with fine elongated, pancaked grains may provide some improvement in resistance to irradiation embrittlement.

The TZM molybdenum also had an elongated, pancaked grain structure, but the grains were larger than observed for the LCAC sheet (Table 5), and TZM has a much higher carbon content with relatively coarse carbides. Fracture initiation in non-irradiated TZM has been shown to occur at carbides [39], which suggests that the carbide precipitates present in TZM could result in the relatively poor resistance to irradiation embrittlement. The coarser grain size and higher carbon content of TZM could also contribute to a higher number density of defects that result in less resistance to irradiation embrittlement, but detailed examinations of microstructure are needed to clarify the differences in DBTT observed for LCAC and TZM after irradiation at 600 °C.

3.3. Post-irradiation tensile properties for irradiation at 936 °C

The tensile properties for LCAC and TZM molybdenum irradiated at 936 °C are compared with results for non-irradiated LSR material and previously reported data for LCAC molybdenum irradiated at 935 °C in Fig. 10. Previous work showed that there was little to no increase in tensile strength for 935 °C irradiated LSR LCAC molybdenum in comparison to thermally conditioned non-irradiated LCAC material that was recrystallized [3]. This indicates that recrystallization of stress-relieved LCAC molybdenum occurred during irradiation, resulting in recovery of the defect structure by the nucleation and growth of new grains to larger size than stress-relieved material, with a concomitant decrease in strength relative to non-irradiated LSR LCAC molybdenum. Irradiation of LCAC molybdenum at 936 °C to higher dose (2.47×10^{26} n/m^2) in this work is expected to result in the formation of coarse voids [1,4,5,18] that result in a small amount of additional irradiation hardening (6–30% increase in tensile strength at room temperature) beyond that observed at the lower dose exposures (1.80 and 4.47×10^{25} n/m^2) with a net

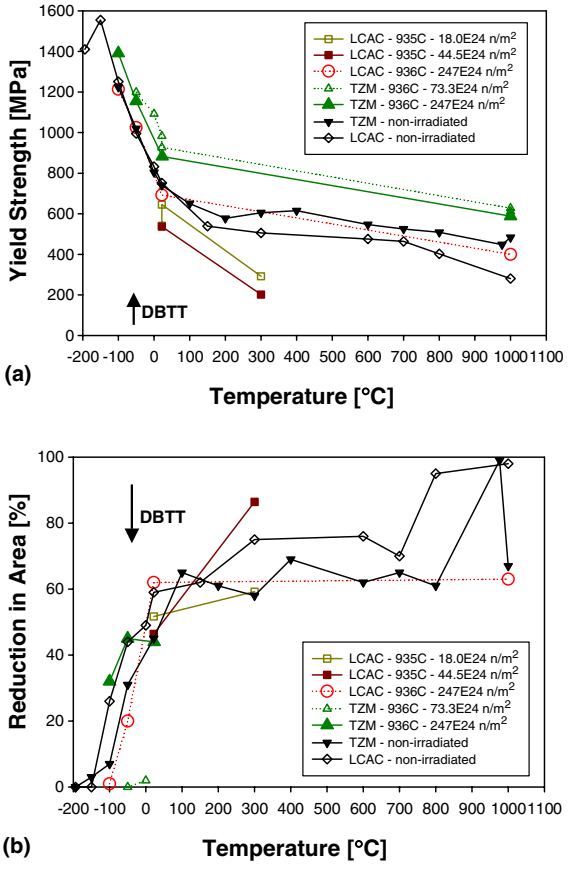

Fig. 10. For irradiations at 936 °C, comparison of non-irradiated and post-irradiated tensile properties for LCAC and TZM molybdenum with some previous results for LCAC [3]: (a) yield strength values and (b) reduction in area values. The yield strength values determined at temperatures below the DBTT are actually a fracture stress in some cases as true plastic deformation has not been achieved.

result of the post-irradiated tensile properties being comparable to non-irradiated LSR LCAC molybdenum tested at −100 °C to room temperature.

Recrystallization of TZM is not expected during the 936 °C irradiations so that the expected formation of coarse voids results in a relatively small increase in yield strength (13–36% increase) with low amounts of irradiation hardening. The yield strength of TZM irradiated to doses of 7.33×10^{25} n/m^2 and 2.47×10^{26} n/m^2 are shown in Fig. 10(a) to be close with a trend for slightly lower strength for the higher dose. This indicates that saturation for the small increase in tensile properties occurs at a fluence of 7.33×10^{25} n/m^2, but irradiation of TZM at 936 °C to higher doses could lead to some recovery of irradiation strengthening.

The load–displacement curves for 1000 °C irradiated LCAC and TZM molybdenum are shown in Fig. 11 to

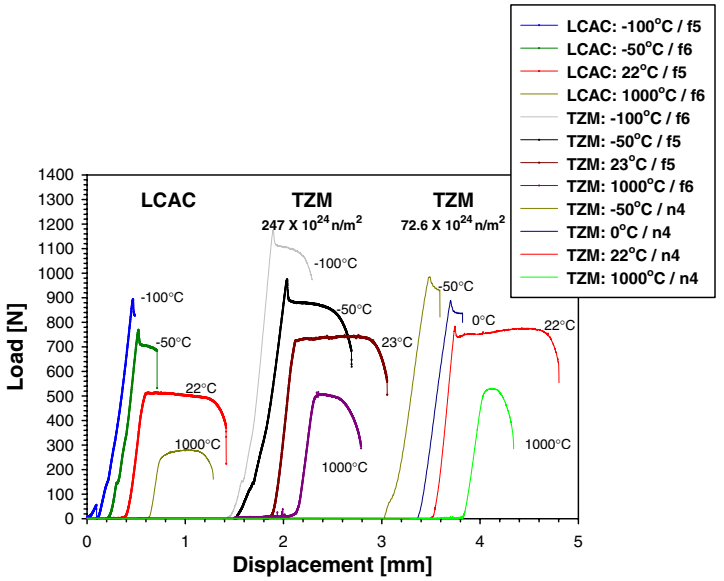

Alloy	LCAC				TZM							
Capsule	f5	f6	f5	f6	f6	f5	f5	f6	n4	n4	n4	n4
Test Temp	-100°C	-50°C	22°C	1000°C	-100°C	-50°C	23°C	1000°C	-50°C	0°C	22°C	1000°C
n	--	-0.058	-0.012	0.090	-0.13	-0.11	0.018	0.042	-0.21	0.08	0.037	0.036

Fig. 11. Plot of load–displacement curves for LCAC and TZM molybdenum in the LSR orientation from tensile testing at −100 °C to 1000 °C following irradiation at 936 °C to a fluence of either 247×10^{24} n/m^2 (f5 and f6) or 73.3×10^{24} n/m^2 (n4). Values for the strain hardening exponents are given, and are summarized in Tables 7 and 8.

be similar to those observed for non-irradiated material (Fig. 2) with the exception of the upper/lower yield point (Lüder's plateau) occurring over a smaller displacement range for sub-ambient testing and a more pronounced Lüder's plateau observed for irradiated TZM at sub-ambient test temperatures. A slight Lüder's plateau is observed for the room temperature tensile test of lower dose (7.33×10^{25} n/m^2) TZM that is absent for the high dose (2.47×10^{26} n/m^2) specimen, which is evidence of a general recovery of defects at higher dose during the 1000 °C irradiations. The strain hardening exponents for 936 °C irradiated LCAC and TZM were slightly lower than non-irradiated for testing at temperatures between room temperature and −100 °C, which indicates that the low number density of coarse voids that would be expected to be formed during irradiation have only a small effect on the plastic flow properties. The slightly higher tensile strength and larger strain hardening exponents observed for 936 °C irradiated TZM and LCAC relative to non-irradiated for testing at 1000 °C suggests that the defect structure is stable up to temperatures of 1000 °C.

Large amounts of tensile ductility, plasticity in the load–displacement curves, and ductile failure modes were observed for 936 °C irradiated LCAC molybdenum after tensile testing at −50 °C to 1000 °C, while low ductility, linear-elastic load–displacement curve, and a brittle failure mode were observed for LCAC tested at −100 °C, see Fig. 12(a) and (b). The ductile failure mode observed for 936 °C irradiated LCAC at temperature/−50 °C was a mixed-mode failure consisting of ductile-laminate features and transgranular cleavage, which is similar to that observed for LCAC irradiated at 935–1100 °C to a lower dose [3]. This indicates that the DBTT for 936 °C irradiated LCAC is −50 °C, which represents a small increase from the −100 °C DBTT observed for non-irradiated LCAC. The brittle failure mode observed for 936 °C irradiated LCAC at −100 °C consists of cleavage with regions of transgranular failure and intergranular features across larger, equiaxed grains. Recrystallization of LCAC during the 936 °C irradiation results in an increase in grain size that likely produces the increase in DBTT from −100 °C to −50 °C, and the formation of larger grains results in intergranular features at the fracture surface.

For the 936 °C irradiation of TZM to the lower dose of 7.33×10^{25} n/m^2, small amounts of tensile elongation, plasticity in the load–displacement curves, and local regions of ductility were observed for tensile testing at 0 °C and room temperature, which indicates that the DBTT was 0 °C. Similar results were observed in both the longitudinal and transverse orientations. Irradiation of TZM at 936 °C to the higher dose of 2.47×10^{26} n/m^2 results in high ductility, measurable plasticity observed

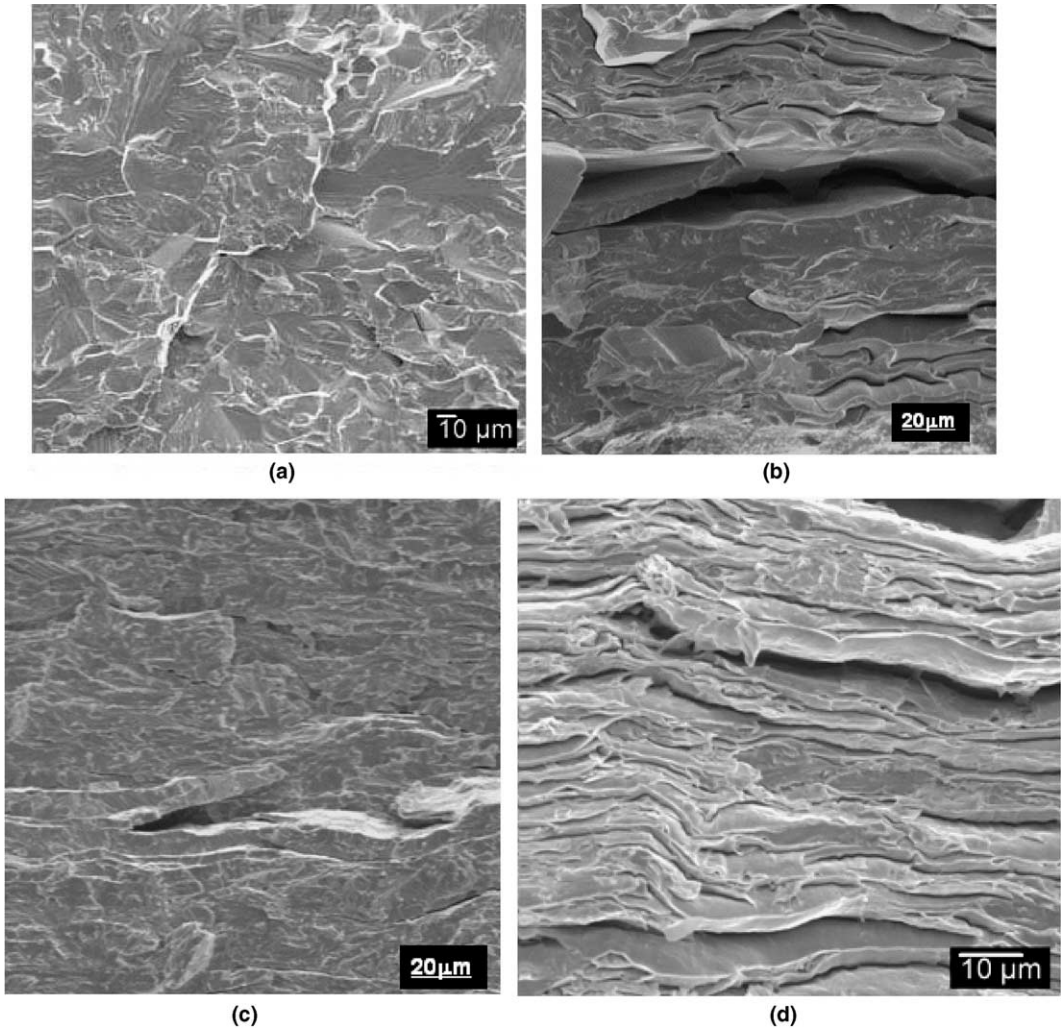

Fig. 12. Post-irradiated SEM fractography of TZM and LCAC molybdenum following 936 °C irradiations to 2.47×10^{26} n/m^2 for tensile testing of (a) LCAC tested at −100 °C, (b) LCAC tested at room temperature, (c) TZM tested at −100 °C, and (d) TZM tested at −50 °C.

in the load–displacement curves, and ductile failure modes observed at temperatures ranging from −50 °C to 1000 °C, while low tensile ductility and brittle behavior were observed for TZM at −100 °C, see Fig. 12(c) and (d). This indicates that irradiation of TZM at 936 °C to higher dose may result in a small decrease in DBTT from 0 °C to −50 °C due to recovery during the 936 °C irradiations, but this likely represents some scatter in tensile results at test temperatures near the DBTT. The DBTT for 936 °C irradiated TZM is identified as −50 °C, which is the same as observed for non-irradiated TZM, see Table 6. Since recrystallization of TZM is not expected to occur during the 936 °C irradiations, the only microstructural change to take place is the development of a low density of clusters which results in minimal hardening with no effective change in the DBTT. The results indicating no change in DBTT for TZM with only slight irradiation hardening indicate that changes in microstructure during irradiation, such as the recrystallization observed for LCAC, are not desired, and more attractive properties are observed for alloys that are microstructurally stable at the 936 °C irradiation temperature, such as TZM or LCAC in recrystallized starting condition [3]. The DBTT values for TZM and LCAC irradiated at 936 °C are shown in Fig. 9 to be lower than the limited results reported in literature, which indicates that irradiation at 936 °C, where the formation of a low number density of coarse voids is expected, results in little change in tensile properties. The lower post-irradiated DBTT values for the LCAC

and TZM evaluated here may result from the lower impurity contents of molybdenum alloys typically being produced today.

4. Summary

Irradiation of LCAC and TZM molybdenum at 300 °C and 600 °C to fluences of 12.3–13.1 dpa results in large increases in tensile strength, which are comparable for each alloy and irradiation temperature. Saturation of the increase in tensile strength was observed to occur at a fluence of 1.05×10^{25} n/m^2 for the 300 °C irradiations, while a higher dose of 7.26×10^{25} n/m^2 was required for saturation in the 600 °C irradiations. This can be explained by the higher number density of smaller loops and voids expected to result from the 300 °C irradiations leading to formation of a stable distribution of obstacles that limits dislocation motion at much lower dose (shorter time) than required for the coarser void structure produced by the 600 °C irradiations. Although differences in microstructure and size and spacing of defects are expected for the 300 °C and 600 °C irradiations, the similarity in tensile strength values at saturation dose indicates that the defect structures are equally effective barriers to dislocation motion, and the true yield stress at temperatures below the DBTT is elevated to a level well above the effective fracture stress of the material so that the tensile stress values being measured are actually a fracture stress. Since fracture stress is a function of flaw size and the inherent toughness of the material, comparable tensile stress values would be expected when the effective yield stress is elevated well above the effective fracture stress of the material, which is apparently the case for 300 °C and 600 °C irradiations at saturation.

The DBTT's for 300 °C irradiated LCAC and TZM molybdenum at the highest dose of 2.32×10^{26} n/m^2 were both determined by tensile tests to be 800 °C, which represents a small increase from the 600 °C DBTT previously determined at a lower dose (1.05×10^{25} n/m^2). The DBTT's of 600 °C irradiated LCAC and TZM were determined to be 300 °C and 700 °C, respectively. The finer grain size of LCAC with lower interstitial content likely explains the improved resistance to irradiation embrittlement compared to TZM and the majority of literature data for molybdenum alloys. TZM has higher carbon content and coarse carbide precipitates that may serve as fracture initiation sites, which may explain the relatively poor resistance to irradiation embrittlement.

Irradiation of LSR LCAC molybdenum to a high fluence (2.47×10^{26} n/m^2) at 936 °C results in recrystallization that produces an increase in grain size with a decrease in tensile strength and a small amount of hardening that results in no net change in strength relative to non-irradiated material. The DBTT for 936 °C irradiated LCAC is observed to slightly increase from −100 °C for non-irradiated to −50 °C for irradiations to the highest dose, but this small increase in DBTT may be attributable to the increase in grain size resulting from recrystallization rather than the effects of irradiation or point defect clusters. Irradiation of TZM at 936 °C produces a small increase in tensile strength, but recrystallization is not observed and this limited increase in strength is observed even after high dose (2.47×10^{26} n/m^2) with saturation of strengthening observed after a dose of 7.33×10^{25} n/m^2. No change in DBTT was observed for 936 °C irradiated TZM relative to non-irradiated with a post-irradiated DBTT of −50 °C. This can be attributed to the stability of the grain size of TZM at this temperature, as shown in other studies. Irradiation of molybdenum alloys at temperatures >800 °C results in the formation of a low number density of coarse voids that apparently have little influence on the tensile properties.

Acknowledgements

This work was supported under USDOE Contract No. DE-AC11-98PN38206. The careful and timely review of this work by W.L. Ohlinger is much appreciated. Thanks to the following ORNL personnel for completing the irradiations, tensile testing and fractography (J.P. Strizak, T.S. Byun, A.L. Qualls, A.W. Williams, and J.L. Bailey).

References

[1] V.K. Sikka, J. Moteff, Nucl. Technol. 22 (1974) 52.
[2] S.J. Zinkle, N.M. Ghoniem, Fusion Eng. Des. 51&52 (2000) 55.
[3] B.V. Cockeram, J.L. Hollenbeck, L.L. Snead, J. Nucl. Mater. 324 (2004) 77.
[4] B.L. Cox, F.W. Wiffen, J. Nucl. Mater. 85&86 (1979) 901.
[5] F.W. Wiffen, in: R.J. Arsenault (Ed.), Proceedings of the 1973 International Conference on Defects and Defect Clusters in B.C.C. Metals and Their Alloys, Nuclear Metallurgy, vol. 18, 1973, p. 176.
[6] R.E. Gold, D.L. Harrod, J. Nucl. Mater. 85&86 (1979) 805.
[7] A. Hasegawa et al., J. Nucl. Mater. 233–237 (1996) 565.
[8] B.N. Singh et al., J. Nucl. Mater. 212–215 (1994) 1292.
[9] Standard Specification for Molybdenum and Molybdenum Alloy Plate, Sheet, Strip, and Foil, ASTM B386-95, American Society for Testing and Materials, Philadelphia, PA, 1997.
[10] M. Semchyshen, R.Q. Barr, J. Less Common Met. 11 (1966) 1.
[11] J. Wadsworth, T.G. Nieh, J.J. Stephens, Scripta Met. 20 (1986) 637.
[12] A. Kumar, B.L. Eyre, Proc. R. Soc. Lond. A 370 (1980) 431.

[13] H. Kurishita, H. Yoshinaga, Mater. Forum 13 (1989) 161.
[14] W.D. Klopp, J. Less Common Met. 42 (1975) 261.
[15] A. Lawley, J. Van den Sype, R. Maddin, J. Inst. Met. 91 (1962–1963) 23.
[16] B.V. Cockeram, Metall. Trans. 36A (2005) 1777.
[17] B.V. Cockeram, Metall. Trans. 33A (2002) 3685.
[18] V.K. Sikka, J. Moteff, J. Nucl. Mater. 54 (1974) 325.
[19] K. Watanabe et al., J. Nucl. Mater. 258–263 (1998) 848.
[20] V. Chakin, V. Kazakov, J. Nucl. Mater. 233–237 (1996) 570.
[21] K. Abe et al., J. Nucl. Mater. 122–123 (1984) 671.
[22] K. Abe et al., J. Nucl. Mater. 99 (1981) 25.
[23] M. Scibetta, R. Chaouadi, J.L. Puzzolante, J. Nucl. Mater. 283–287 (2000) 455.
[24] T.H. Webster et al., in: Proceedings of BNES Conference on Irradiation Embrittlement and Creep in Fuel Cladding and Core Components, 9–10 November 1972, pp. 61.
[25] I.V. Gorynin et al., J. Nucl. Mater. 191–194 (1992) 421.
[26] A. Hasegawa et al., J. Nucl. Mater. 225 (1995) 259.
[27] H.H. Smith, D.J. Michel, J. Nucl. Mater. 66 (1977) 125.
[28] K. Furuya, J. Moteff, Metall. Trans. 12A (July) (1981) 1303.
[29] J.A. Sprague et al., J. Nucl. Mater. 85&86 (1979) 739.
[30] B. Mastel, J.L. Brimhall, Acta Metall. 13 (1965) 1109.
[31] B.V. Cockeram, J.L. Hollenbeck, L.L. Snead, J. Nucl. Mater. 336 (2005) 299.
[32] J.A. Shields, P. Lipetzky, A.J. Mueller, in: G. Kneringer, P. Rodhammer, H. Wildner (Eds.), Proceedings of the 15th International Plansee Seminar, vol. 4, Plansee Holding AG, Reutte, Austria, 2001, p. 187.
[33] L.L. Snead, S.J. Zinkle, Nucl. Instrum. and Meth. B 191 (2002) 497.
[34] L.R. Greenwood, F.A. Garner, J. Nucl. Mater. 212–215 (1994) 635.
[35] Standard Test Methods for Tension Testing of Metallic Materials, ASTM E8-01, American Society for Testing and Materials, Philadelphia, PA, 2001.
[36] L.R. Greenwood, R.K. Smither, Specter: Neutron Damage Calculations for Materials Irradiations, ANL/FPP/TM-197, Argonne National Laboratory, January 1985.
[37] K.S. Chan, Metall. Trans. 20A (1989) 155.
[38] K.S. Chan, Metall. Trans. 20A (1989) 2337.
[39] J. Wadsworth, C.M. Packer, P.M. Chewey, W.C. Coons, Metall. Trans. 15A (1984) 1741.